

CHAPTER 10. Magnetic Measurements.

1. Introduction

Nine short models (HGQ01-HGQ09) of approximately 2 m length have been fabricated. Eight of them have been tested in superfluid helium at the Fermilab Vertical Magnet Test Facility. Magnet transfer function and field harmonics have been measured in the magnet straight section and in the end regions. In this section we present results of the measurements and compare them with calculations based on as-built magnet geometry and with preliminary field quality specifications.

2. Magnetic Design Update

The magnet design is based on four two-layer coils connected in series, surrounded by collar and yoke laminations. No significant modifications to the design cross-section for these magnets were made during the magnet model program, but various coil shimming schemes have been implemented in the models to obtain the desired coil prestress.

The end regions underwent several design iterations during the model program. The first five models were built with a four-block end configuration. With respect to the design of HGQ01, the second-wound group of the outer coil was shifted by 2 cm in the positive z direction starting with HGQ02 to reduce the peak field in the coil. A more compact design for the coil to coil joint in the lead end was introduced in HGQ03 and HGQ05. A new five-block configuration was implemented in models beginning with HGQ06 which improves the mechanical stability of inner layer conductors during winding. The new design also reduces the peak field in the coil and significantly improves field quality in the end region.

The model magnet collar and yoke design allows for use of tuning shims to correct field errors. Shims are located in 8 rectangular cavities between the collars and yoke. In magnets HGQ01-05, these cavities were filled with a nominal shim package of half magnetic and half non-magnetic material. Shim motion as magnet current was ramped generated voltage spikes in quench detection signals and changes in field harmonics so the cavities were left empty in magnets HGQ06 and 07. For HGQ08 and HGQ09 the iron yoke cross-section was re-optimized (smaller round holes, no magnetic shims).

3. Field Quality Analysis and Magnetic Measurement System

In the straight section of the magnet, the field is represented in terms of harmonic coefficients defined by the power series expansion

$$B_y(x, y) + iB_x(x, y) = 10^{-4} B_2 \sum_{n=1}^{\infty} (b_n + ia_n) \left(\frac{x + iy}{R_{ref}} \right)^{n-1},$$

where $B_x(x, y)$ and $B_y(x, y)$ are the transverse field components, B_2 is the quadrupole field strength, b_n and a_n are the $2n$ -pole coefficients ($b_2=10^4$) at a reference radius R_{ref} of 17 mm.

The coordinate system for magnetic measurement is defined with the z -axis at the center of the magnet aperture and pointing from return to lead end with the origin at the boundary between return end and straight section. The x -axis is horizontal and pointing right, and the y -axis, vertical and pointing up to the observer who faces the magnet lead end.

Magnet transfer function, magnetic length and magnet twist were determined according the following definitions:

- Transfer function G/I : $B_2^{body} / R_{ref} I$, $A_2 \equiv 0$, where B_2^{body} and A_2 are the “normal” and “skew” quadrupole field strength in magnet body at the reference radius, R_{ref} is reference radius and I is current in the coil.
- Magnetic length: $L_{mag} \equiv \int B_2 dl / B_2^{body}$.
- Magnet twist: $\Delta\Phi_2 / \Delta z$ in the magnet body, where Φ_2 is the quadrupole phase relative to an angular encoder (arbitrary zero) and z is the longitudinal coordinate. Mechanical measurements of cold mass twist are made as described in Chapter 4.

Magnetic measurements were performed using a vertical drive, rotating coil system. Probes used have a tangential winding for measurement of higher order harmonics as well as specific dipole and quadrupole windings for measurement of the lowest order components of the field. These windings also allow for bucking the large dipole and quadrupole components in the main coil signal. Most measurements presented were made with a coil of 40.6 mm nominal diameter and length 82 cm. A short probe with 25 mm nominal diameter and 4.3 cm length was used for longitudinal scans of the magnet end regions.

Coil winding voltages are read using HP3458 DVMs. An additional DVM is used to monitor magnet current. DVMs are triggered simultaneously by an angular encoder on the probe shaft, synchronizing measurements of field and current. Feed down of the quadrupole signal to the dipole is used to center the probe in the magnet.

4. Magnetic Parameters

A. Transfer Function

Table 2 reports the measured transfer function in all model magnets, showing good reproducibility and agreement with calculations. The offset in the measured transfer function in magnets HGQ06-08 is due to the testing of these magnets without tuning shims [9] in the allocated slots, once the decision was taken to remove these from the final design. The final yoke design adds the nominal magnetic component of the shim directly to the lamination; and we see the transfer function measured in HGQ09 agrees well with that of early magnets with tuning

shims. Figure 1 compares the measured and predicted transfer function for the magnets as a function of current. Magnets 6/7 and 8 are plotted separately as all had empty tuning shim slots. In addition HGQ08 coils were made of staybrite coated strand.

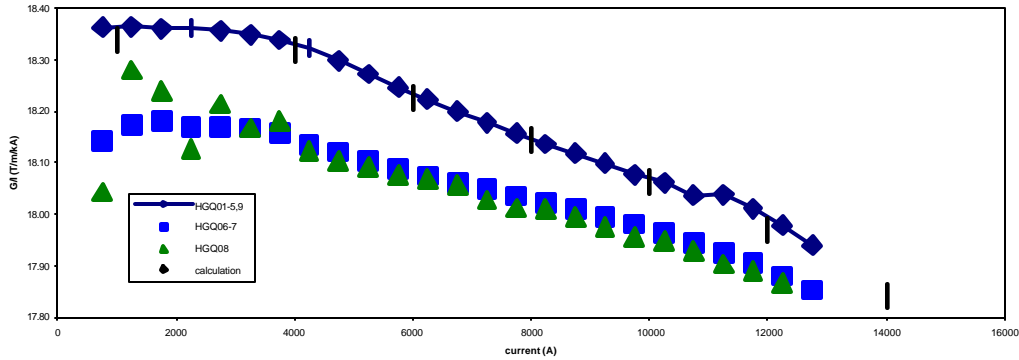


Figure 1. Measured and Calculated (TDH) Magnet Transfer Function

Table 1. Measured Transfer Function

	G/l, T/m/kA							
I, A	HGQ01	HGQ02	HGQ03	HGQ05	HGQ06	HGQ07	HGQ08	HGQ09
750	18.375	18.338	18.361	18.381	18.139	18.147	18.043	18.391
5750	18.231	18.221	18.229	18.270	18.101	18.076	18.075	18.303
10750	18.011	18.023	18.007	18.051	17.960	17.931	17.929	18.092

B. Magnetic Length Measurements

The magnetic length of two magnets was measured in various ways. HGQ05 and HGQ09 were measured with SSW warm with 10 A excitation. Integral scans of HGQ09 were made with both a long (0.8 m) and short (0.04 m) probe at 6 kA cold. Magnetic length measurements are summarized in Table 3. The ratio of magnetic and geometric lengths is given in Table 4.

Table 2. Magnetic Length Measurements

	probe	I (kA)	Lmag	error
HGQ09	long	12.5	1.780	0.003
		11	1.778	0.000
		6	1.771	0.001
		6	1.778	0.004
	short	6	1.776	0.001
HGQ05	SSW	warm		
	SSW	warm	1.786	0.003

Table 3. Ratio of Magnetic and Geometric Lengths

		Lmag	Lgeom	ratio
HGQ05	SSW	1.786	1.866	0.96
HGQ09	high current	1.779	1.847	0.96
	low current	1.775	1.847	0.96
	SSW		1.851	0.00

C. Field Angle (Magnet Twist)

A large variation (7-8 mrad/m) in the measured field angle along the length was measured in HGQ01 (Fig. 2). The large change in the lead end relative to the body is also consistent with the skew quadrupole present. A relatively large change in the return end field relative to the body was also indicated. This would not be so surprising as the return end is not locked to the straight section azimuthally. Mechanical measurements subsequently confirmed this large twist of the cold mass in the straight section of the magnet.

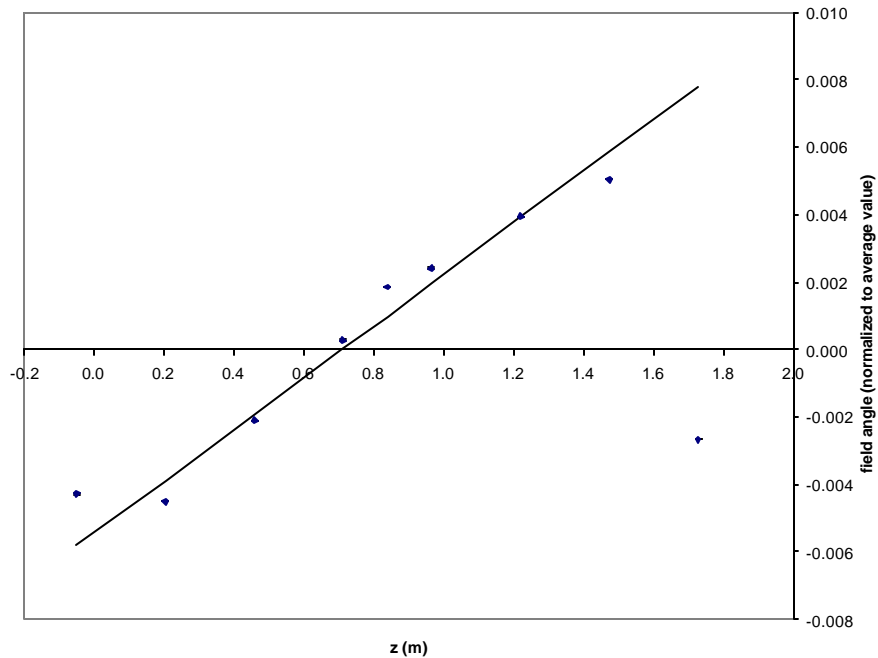


Figure 2. Field angle change along the magnet (HGQ01)

Mechanical measurements of the twist and magnetic measurements of the field angle as a function of longitudinal position were made for all magnets, but a reduction in twist by tooling alignment and yoke/skin welding procedure optimization (see Chapter 4) quickly reduced twist below the level which could be reliably measured by magnetic measurement equipment¹ although mechanical and magnetic measurements are consistent for all magnets (Table 2). Twist reduction below our goal of 0.2 mrad/m was achieved in HGQ07 and subsequent magnets.

¹ A survey of the measurement rig indicated as much as 1 mrad angular twist in the apparatus. It is unlikely to be this large, but it can not be ruled out.

Table 4. Summary of Magnet Mechanical and Magnetic Twist Measurements

Model number	Mechanical twist, mrad/m	Magnetic twist, mrad/m
HGQ01	4.7	8
HGQ02	0.6	<1
HGQ03	1.0	
HGQ05	0.9	
HGQ06	1.0	
HGQ07	0.2	
HGQ08	0.1	
HGQ09	0.1	

5. Field Harmonics

A. Magnet body (straight section) harmonics

As was reported previously [4], large values for both allowed and unallowed harmonics were measured in HGQ01 due to the thick coil shims (up to 450 microns) needed to obtain the required pre-stress, affecting b_6 and b_{10} , and differences in coil sizes (80 microns) in the different quadrants, producing a_4 and a_8 . Significant improvements have been made in fabrication procedures [5]. Better uniformity in coil size and modulus has been achieved which has led to corresponding improvement in field quality from magnet to magnet.

Table 6 shows a comparison between measured harmonics and calculations based on as-built parameters for the harmonic components b_6 , b_{10} , a_4 and a_8 . Calculations and measurements are generally in good agreement. The measurements are made at a current of 6 kA where all non-geometric components (conductor magnetization, iron saturation, conductor displacement under Lorentz forces) are small. A reduction of the errors of about one order of magnitude is observed from magnet HGQ01 to magnet HGQ05. In magnets HGQ05, all four harmonics are within the uncertainties specified by the reference table. Calculated values for these components of the field based on as-built parameters are similarly small in HGQ06-HGQ09.

Table 5. Comparison of Measured Body Harmonics with Calculations at I=6 kA

Field harmonics	HGQ							
	01	02	03	05	06	07	08	09
b_6 , calc.	-4.24	-2.86	-1.39	-0.08	-	-	-	-
b_6 , meas.	-3.91	-1.54	-1.02	-0.30	-0.05	-0.45	-0.06	-0.28
b_{10} , calc.	-0.14	-0.09	-0.04	0.01	-	-	-	-
b_{10} , meas.	-0.10	-0.10	-0.04	0.01	0.00	-0.02	-0.01	-0.01
a_4 , calc.	1.27	0.94	0.00	0.00	-	-	-	-
a_4 , meas.	2.00	0.53	0.32	0.19	-0.31	-0.50	-0.44	0.31
a_8 , calc.	0.02	0.00	0.00	0.00	-	-	-	-
a_8 , meas.	0.02	0.02	0.03	0.00	0.00	0.01	-0.01	0.01

Table 6. Measured Marmonics in the Magnet Straight Section at I=6 kA.

As Measured Harmonics								
	HGQ01	HGQ02	HGQ03	HGQ05	HGQ06	HGQ07	HGQ08	HGQ09
b3	0.36	-0.70	1.04	0.72	0.25	0.18	0.61	0.71
a3	0.27	0.55	-0.30	0.12	-0.27	0.41	-0.01	0.35
b4	0.26	0.18	0.14	0.00	0.09	0.01	-0.12	-0.05
a4	2.00	0.53	0.32	0.19	-0.31	-0.50	-0.44	0.31
b5	-0.29	0.09	-0.34	-0.04	-0.11	-0.04	-0.01	0.08
a5	0.02	-0.17	0.26	0.05	-0.07	-0.24	0.12	-0.14
b6	-3.91	-1.54	-1.02	-0.30	-0.05	-0.45	-0.06	-0.28
a6	-0.02	0.03	0.07	-0.03	-0.05	-0.10	-0.03	0.04
b7	-0.08	-0.01	-0.06	0.01	-0.03	0.02	-0.01	0.06
a7	-0.05	0.00	-0.03	0.01	0.00	0.08	0.00	0.02
b8	0.06	0.01	0.00	0.00	0.00	0.00	0.00	-0.01
a8	0.02	0.02	0.03	0.00	0.00	0.01	-0.01	0.01
b9	0.04	0.00	0.00	0.00	0.00	-0.01	0.00	0.00
a9	0.01	-0.01	0.01	0.00	0.00	0.01	0.01	0.00
b10	-0.10	-0.10	-0.04	0.01	0.00	-0.02	-0.01	-0.01
a10	0.02	0.00	-0.01	0.00	0.00	0.00	0.00	0.00

Table 7 shows the measured straight section harmonics up to the 20-pole for all models. In magnets HGQ05-7, all central harmonics are within one standard deviation of the random error specified in error table v.2.0 (see Introduction). From the values in Table 7, averages and standard deviations over the eight models have been obtained for each component (Table 8). In the attempt to eliminate the effect of systematic errors due to coil shims, the values for b₆, b₁₀, a₄ and a₈ in Table 8 have been obtained after taking the difference between measured values and those calculated based on as-built parameters (Table 6).

Table 8. Averages and standard deviations over the eight models

	All Corrected		Q01-03 Correc		Q05-09 Measu	
	Mean	RMS	Mean	RMS	Mean	RMS
b3	0.35	0.55	0.23	0.88	0.49	0.26
a3	0.11	0.33	0.17	0.43	0.12	0.28
b4	0.08	0.13	0.19	0.06	-0.01	0.08
a4	-0.06	0.48	0.21	0.58	-0.15	0.37
b5	-0.10	0.16	-0.18	0.24	-0.02	0.07
a5	0.00	0.17	0.04	0.22	-0.06	0.15
b6	0.17	0.59	0.67	0.56	-0.23	0.17
a6	-0.02	0.06	0.03	0.04	-0.03	0.05
b7	-0.02	0.04	-0.05	0.04	0.01	0.03
a7	0.00	0.04	-0.03	0.03	0.02	0.03
b8	0.01	0.02	0.02	0.03	0.00	0.01
a8	0.01	0.01	0.02	0.02	0.00	0.01
b9	0.00	0.02	0.01	0.02	0.00	0.00
a9	0.00	0.01	0.00	0.01	0.00	0.01
b10	0.00	0.02	0.01	0.03	0.00	0.01
a10	0.00	0.01	0.00	0.02	0.00	0.00

All average values and standard deviations in Table 8 are within the limits specified in error table. Note the b_6 result is strongly influenced by the relatively large difference between calculation and measurements in a single magnet (HGQ02). Moreover, one can expect smaller variations in a magnet production series than those observed in the first few models of a new design.

The magnet design provides good compensation of the saturation and Lorentz force effect, and the change in the average harmonic value between injection and operating current is very small. In particular, the 6 kA measurements (Table 7) do not differ significantly from those taken at higher currents.

As part of the normal testing cycle, the field is measured during a "pseudo-accelerator cycle" in which the magnet is ramped through a series of pre-cycles, brought to injection current and held, then ramped to flat top. Table 9 summarizes the change in b_6 at injection measured in the model magnets. Note that we expect these changes to have negligible impact on machine performance as the number of insertion quadrupoles is a small fraction of all magnets.

Table 9. Change in b_6 at injection.

Dt (sec)		HGQ								average	st. dev.
		1	2	3	5	6	7	8	9		
b_6	0	-1.1	-0.9	-0.6	-1.7	-1.5	-1.5	-1.3	-1.2	-1.2	0.4
Δb_6	900	< 0.1	0.9	0.7	0.4	0.6	0.2	0.2	0.3	0.4	0.3
	1773		1.0	0.7	0.4	0.7	0.2	0.3	0.3	0.4	0.3

Figure 3 shows the measured dodecapole in model HGQ05 along with calculations of geometric and dynamic effects. The magnet design provides good compensation of the saturation and Lorentz force effect, and the total change of the mean dodecapole between injection and operating current is very small. This is actually the case for all harmonics. In particular, the 6 kA measurements (Table 7) do not differ significantly from those taken at higher currents. A simulation of the conductor magnetization effect on the normal dodecapole agrees very well with HGQ05 measurements, assuming a systematic (geometric) shift of -0.3 units. The magnetization effect is similar for all magnets, as expected from the uniformity of conductor properties. One exception is a specific pattern that appeared in magnet HGQ02 and HGQ03 and which shows a larger effect on the first cycle after quench than during subsequent cycles.

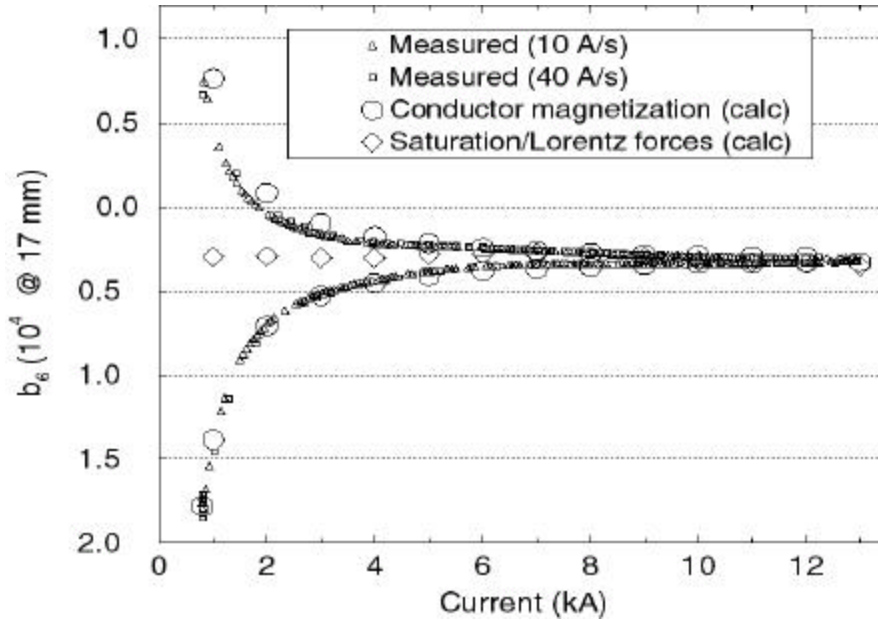


Figure 3. Normal Dodecapole vs Current (HGQ05)

The difference between harmonics measured during down and up ramp was small in magnets HGQ01-5, indicating small magnetization and eddy current effects [7]. However, in magnets HGQ06-08, large differences between harmonics measured during up and down ramps were seen. These differences increased with increasing ramp rate (Table 10).

Table 10. Difference between Field Harmonics Measured on the Up and Down Ramp in HGQ06 at I=6kA.

<i>ramp rate</i>	10 A/s		80 A/s	
	Δb_n	Δa_n	Δb_n	Δa_n
3	-0.94	-0.43	-6.67	-3.57
4	-0.16	-0.03	-1.19	0.11
5	0.12	0.11	0.86	0.61
6	0.20	-0.03	2.07	-0.23
7	-0.04	-0.01	-0.27	-0.11
8	0.00	0.00	0.00	0.00
9	0.01	0.00	0.06	-0.02
10	-0.01	0.00	-0.06	-0.02

These ramp rate dependent field effects are due to eddy currents in the magnet coils. Effects seen in the measured fields for these two magnets are consistent with measurements of energy losses during AC cycling of magnet power [8]. Analysis shows that the eddy currents are due to low and varying crossover resistances in the coils of these magnets caused by changes in the coil curing temperature and pressure. In particular, magnets HGQ06 and 07 were the only ones in which the coils were cured at both high temperature and pressure (Table 11). Predictions for

crossover resistance values based on the measured harmonics for HGQ06 show low resistance values and large variations from coil to coil, which also explains the non-allowed ramp dependent multipole components.

Table 117. Effect of Coil Curing Cycle on Eddy Current Effects in HGQ Short Models

Model #	Coil curing cycle		I _c (300A/s), A	Δb ₆ (40 A/s) @6kA, 10 ⁻⁴
	Temperature, °C	Pressure		
HGQ01	135	low	10965	0.02
HGQ02	190	low	11335	0.21
HGQ03	195	low	11298	0.16
HGQ05	130	low	10519	0.12
HGQ06	190	high	6433	-1.04
HGQ07	190	high	4487	-0.55
HGQ08	190	high	3941	-0.72
HGQ09	190/135	low/high	12946	0.13

B. End harmonics

End field calculations and measurements of HGQ01-03 were reported in [4,5]. Magnetic measurements of the HGQ06 lead end, which has the new 5-block design, have been performed at a sequence of positions along the *z* axis, in steps of 4.3 cm to match the winding length. Due to the presence of a longitudinal field component, and to the dependence of the transfer function on the longitudinal position, the local end field is best described in terms of field integrals over the probe length, at the probe radius. A comparison between calculated and measured B₂ is shown in Figure 4.

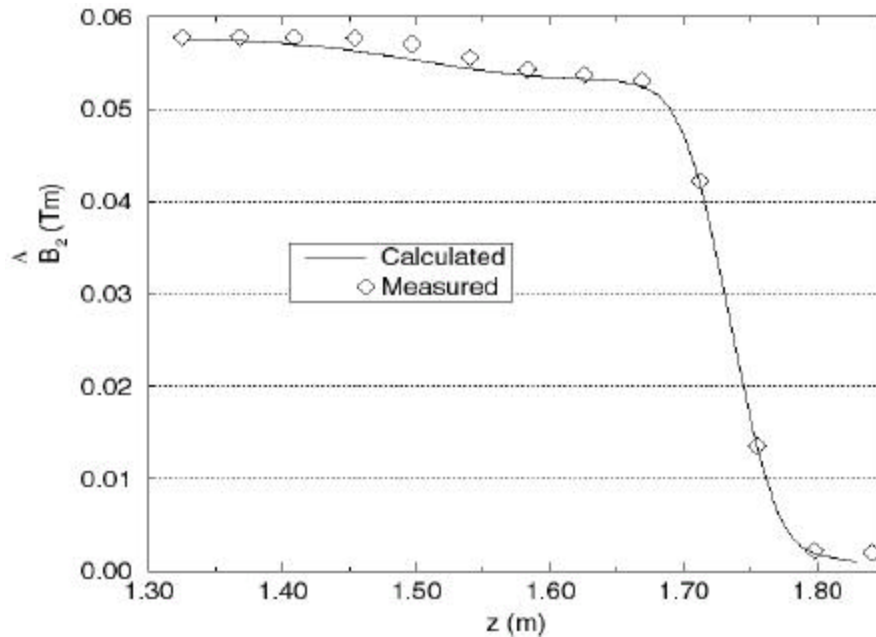


Figure 4. Normal Quadrupole in HGQ06 Lead End

As in the magnet straight section, the integrated multipole components in the end regions are expressed in units of 10^{-4} of the main integrated quadrupole field. The magnetic length L_m of the interval is defined as the length of straight section which would provide an equivalent integrated gradient. The reference integration interval in z for harmonic coefficients in the magnet ends is defined to be $[-0.57, 0.25]$ m for the return end and $[1.31, 2.13]$ m for the lead end, matching the length of the measurement probe [9].

Table 82. Harmonics in the Magnet Lead End

Field harmonics	HGQ							
	01	02	03	05	06	07	08	09
b_6 , calc.	3.1	5.5	5.4	5.4	3.5			
b_6 , meas.	2.9	4.2	3.8	8.0	3.1	3.1	3.1	3.0
b_{10} , calc.	-0.3	-0.3	-0.4	-0.4	-0.1			
b_{10} , meas.	-0.3	-0.2	-0.4	-0.2	-0.1	-0.1	-0.0	-0.1
a_6 , calc.	0.5	0.4	-0.1	-0.1	-0.7			
a_6 , meas.	0.1	0.2	-0.3	-0.6	-0.4	-0.3	-0.4	-0.4
a_{10} , calc.	-0.1	0.0	0.0	0.0	0.0			
a_{10} , meas.	-0.1	0.0	0.0	0.0	0.0	0.0	0.0	0.0

A comparison of measured and calculated harmonics in the magnet lead end is given in Table 9.² Harmonics are calculated using the program ROXIE [10]. For magnet HGQ02 and HGQ03, which used soft ULTEM end parts, thick mid-plane shims were applied to reach the desired pre-stress, resulting in a negative contribution to the dodecapole. In HGQ05, which uses G10 end parts, the thickness of the end shims was substantially reduced. This change in end shims, together with the reduction of the negative contribution from the straight section b_6 , contributes to the positive jump in the measured dodecapole of HGQ05 with respect to HGQ03. With the new 5-block end design implemented in HGQ06, a reduction in b_6 of 35% was achieved.

6. Field Correction

A. Warm/cold correlation

Figure 5 shows the correlation ((cold-warm)/cold) between warm and cold measurements of magnets 2-8. In general the difference is small. There are statistically significant differences between warm and cold measurements of allowed harmonics b_6 and b_{10} on the order of a few

²Except for HGQ01, for which a correction of -2 units was applied to the calculated b_6 integral for HGQ01 to include the contribution of mid-plane shims, the end harmonics quoted in Table are computed for the design geometry without considering the effect of coil shims.

sigma. The differences between warm or cold measurements performed on the same magnet at different stages of the test program are much smaller.

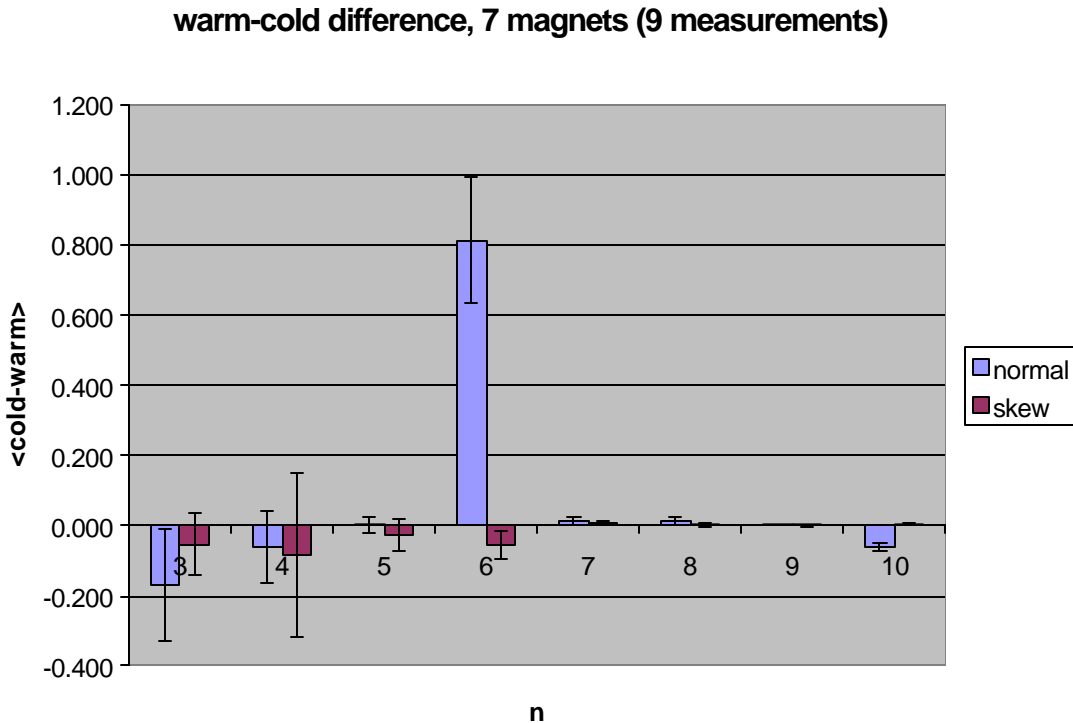


Figure 5 Warm-Cold Correlation

B. Field correction

A method for correction of low order harmonics using magnetic shims has been investigated as part of the HGQ short model program. Results of studies of field correction in these magnets with tuning shims are reported in [2].

Magnetic shims were located in eight rectangular cavities between the yoke inner surface and the collars. Each shim is a package of magnetic (low-carbon steel) and nonmagnetic (brass or stainless steel) laminations. By adjusting the relative thickness of magnetic and nonmagnetic laminations, it is possible to correct random field errors generated by conductor positioning errors.

Correction of individual sextupole and octupole components at nominal current up to several units are possible, with small effect on all other harmonics. Simultaneous corrections of all four sextupole and octupole components up to ± 1.5 units are also possible. The effect on other harmonics is small. Uncertainty in determining the final magnet harmonics based on warm magnetic measurements of the collared coil limit the accuracy of the magnetic shim correction to about one unit.

Results from the HGQ short model program indicate that magnetic shim correction is not required to achieve the specified field quality. For this reason, in order to simplify magnet

fabrication it was decided not to implement the magnetic shim correction scheme during HGQ production. The shape of the yoke lamination was then modified to correspond to the nominal shim thickness.

7. Summary

Magnetic measurements of MQXB short models confirm design calculations for geometric harmonics, magnetization and Lorentz force effects. Refinements in magnet fabrication have significantly improved the field quality in the last three magnets which have systematic and random values of the harmonics in the straight section that are within specifications. An improvement in end field quality has been made by implementing a new 5-block design. Current-dependent effects measured in early magnets were small, but large eddy current effects have been observed in HGQ06 and 07 due to changes in coil curing parameters. This problem was fixed in HGQ09 and production magnets by optimizing coil curing cycle (pressure and temperature).

Table 1 shows the reference harmonics at injection and collision for MQXB magnets (version 3.0) developed based on the results obtained in HGQ short models. For each harmonic component, values of the mean, uncertainty in mean and standard deviation are listed. This table is a reference for the analysis of machine performance and IR systems layout. Preliminary results of beam tracking studies aimed at evaluating the impact of magnet field errors on LHC dynamic aperture indicate that the values listed in Table 1 are acceptable from the machine performance standpoint [3]. Based on the data presented in Table 1 a field quality specification for magnet production will be formulated.

Table 9. Reference Harmonics Table V3.0 for the MQXB. For injection conditions, only geometric and persistent current effects are included

Magnet Body Harmonics (units, $r_{ref} = 17$ mm)

	Collision Energy			Injection Energy		
	Mean	Uncert	Random	Mean	Uncert	Random
b3	0	0.60	0.27	0	0.60	0.27
a3	0	0.23	0.27	0	0.23	0.27
b4	0	0.15	0.27	0	0.15	0.27
a4	0	0.20	0.27	0	0.20	0.27
b5	0	0.15	0.10	0	0.15	0.10
a5	0	0.15	0.10	0	0.15	0.10
b6	0	0.45	0.20	-0.84	0.60	0.20
a6	0	0.07	0.03	0	0.07	0.03
b7	0	0.04	0.02	0	0.04	0.02
a7	0	0.03	0.02	0	0.03	0.02
b8	0	0.008	0.020	0	0.008	0.020
a8	0	0.008	0.010	0	0.008	0.010
b9	0	0.008	0.010	0	0.008	0.010
a9	0	0.008	0.010	0	0.008	0.010
b10	0	0.008	0.010	0	0.008	0.010
a10	0	0.008	0.010	0	0.008	0.010

Magnet End Integrated Harmonics, Injection or Collision Energy
(unit-m, $r_{ref} = 17$ mm)

	Lead End			Return End		
	Mean	Uncert	Random	Mean	Uncert	Random
A2	16.4					
B6	0.82	0.82	0.31	0	0.41	0.31
A6	0	0.21	0.06			
B10	-0.08	0.08	0.04	-0.08	0.08	0.04
A10	0	0.04	0.04			

REFERENCES

- [1] "LHC Conceptual Design", CERN AC/95-05 (LHC).
- [2] G. Sabbi et al., "Correction of High Gradient Quadrupole Harmonics with Magnetic Shims", MT16.
- [3] J. Wei et al., 1999 Particle Accelerator Conference, New York, April 1999.
- [4] R. Bossert et al., "Analysis of Magnetic Measurements of Short Model Quadrupoles for the LHC Low-beta Insertions", EPAC'98, Stockholm, June 1998.
- [5] R. Bossert et al., "Magnetic Measurements of the Fermilab High Gradient Quadrupoles for the LHC Interaction Regions", IEEE Transactions on Applied Superconductivity, Vol. 9, No. 7, June 1999.
- [6] N. Andreev et al., "Study of Kapton Insulated Superconducting Coils Manufactured for the LHC Inner Triplet Model Magnets at Fermilab", MT16.
- [7] N. Andreev et al., "Field Quality of Quadrupole R&D Models for the LHC IR", 1999 Particle Accelerator Conference, New York, April 1999.
- [8] N. Andreev et al., "Quench Behavior of Quadrupole Model Magnets for the LHC Inner Triplets at Fermilab", MT16.
- [9] G. Sabbi et al., "Magnetic Field Analysis of the First Short Models of a High Gradient Quadrupole for the LHC Interaction Regions", Proc. MT-15 Conf., Beijing, 1997.
- [10] S. Russenschuck, Proc. ACES Symposium, Monterey, 1995.